On the current status of OZI violation in πN and pp reactions⋆

A. Sibirtsev, W. Cassing

Institut für Theoretische Physik, Universität Giessen, 35392 Giessen, Germany

Abstract. The available data on ω and ϕ production from πN and pp collisions are reanalyzed with respect to an OZI rule violation on the basis of transition matrix elements. The data are found to be compatible with a constant ratio R, which however, deviates substantially from the SU(3) prediction based on the present knowledge of the $\phi-\omega$ mixing angle.

PACS. 12.10.Kt Unification of couplings – 12.40.Vv Vector-meson dominance – 13.75.Cs Nucleon-nucleon interactions – 13.75.Gx Pion-baryon interactions

1 Introduction

Assuming the ideal SU(3) octet-singlet mixing Okubo, Zweig and Iizuka proposed [1–3] that the production of a ϕ-meson from an initial non-strange state is strongly suppressed in comparison to ω-meson production. Indeed, because of SU(3) breaking the octet and singlet states are mixed and for an ideal mixing angle θ_V=35.3⁰ the ϕ-meson is a pure s$\bar{\text{s}}$ state. In case of ϕ production from πN, NN or N$\bar{\text{N}}$ reactions the OZI rule states that the contribution from the diagram with a s$\bar{\text{s}}$ pair disconnected from the initial u, d, $\bar{\text{u}}$, $\bar{\text{d}}$ should ideally vanish. The experimental deviation from the ideal mixing angle $\Delta\theta_V$=3.7⁰ [4] can be used [5] to estimate the ratio R(ϕ/ω)≈4.2×10^{-3} of the cross sections with a ϕ and ω in the final state. This deviation of the experimental ratio R from zero is denoted as OZI rule violation. A large ratio R might indicate an intrinsic s$\bar{\text{s}}$ content of the nucleon since in that case the ϕ-meson production is due to a direct strangeness transfer from the initial to the final state and thus OZI allowed.

The OZI violation problem has lead to a large experimental activity involving different hadronic reactions. Here we perform a systematical data analysis for πN and pp reactions and discuss their theoretical interpretation in context with the most recent data point from the DISTO Collaboration [6].

2 ω and ϕ production in πN reactions

Without involving any theoretical assumption about the production mechanism the data [7] on the total πN→ωN and πN→ϕN cross sections may be analyzed in terms of the corresponding transition amplitudes. The amplitude

for a two-body reaction with stable particles in the final state is related to the total cross section σ as [8]

$$|M_V| = 4 \left[\pi\sigma s\right]^{1/2} \left[\frac{\lambda(s, m_N^2, m_\pi^2)}{\lambda(s, m_N^2, m_V^2)}\right]^{1/4}, \quad (1)$$

where $\lambda(\text{x}, \text{y}, \text{z}) = (\text{x} - \text{y} - \text{z})^2 - 4\text{yz}$, while m_N, m_π, m_V denote the nucleon, pion and vector meson masses, respectively, and s is the squared invariant collision energy. Moreover, we compare the transition amplitudes for ω and ϕ production at the same excess energy $\epsilon=\sqrt{\text{s}}-m_N-m_V$. As was discussed in [9], (1) can be used for the evaluation of the amplitudes for the production of unstable (ω and ϕ) mesons at excess energies $\epsilon>\Gamma_V$, where Γ_V denotes the width of the vector meson spectral function due to its vacuum decay.

Furthermore, due to the experimental set up the π^-p→ωn data from [10] should not be considered as total cross sections, but as differential cross sections σ_{dif} integrated over a given range of the final neutron momentum [9]. Indeed, the π^-p→ωn cross sections given in [10] for different intervals [$q_{\min}, q_{\max}$] of neutron momenta in the center-of-mass system can be related to the transition amplitude M_V as

$$\sigma_{\text{dif}} = \int\limits_{q_{\min}}^{q_{\max}} \frac{|M_V|^2}{4\pi^2 \, \lambda^{1/2}(s, m_p^2, m_\pi^2)} \, \frac{q^2}{\sqrt{q^2 + m_n^2}}$$

$$\frac{\Gamma_V m_V}{(s - 2\sqrt{s(q^2 + m_n^2)} + m_n^2 - m_V^2)^2 - \Gamma_V^2 m_V^2} \, dq, \quad (2)$$

where m_p and m_n are the proton and neutron masses, respectively, and s is given as a function of (2) agrees with that in [9] in the non-relativistic limit. Furthermore, in the calculations we use the set of the neutron momentum intervals [$q_{\min}, q_{\max}$] as in [10].

⋆ Supported by Forschungszentrum Jülich

Figures 1,2 show the transition amplitudes for the $\pi N \rightarrow \omega N$ and $\pi N \rightarrow \phi N$ reactions evaluated from the experimental data [7,10]. Note, that the $\pi^- p \rightarrow \omega n$ transition amplitude evaluated from the data of [10] (full dots at small ϵ) by (2) does not depend on energy within the errorbars and agrees well with that extracted from the other data [7].
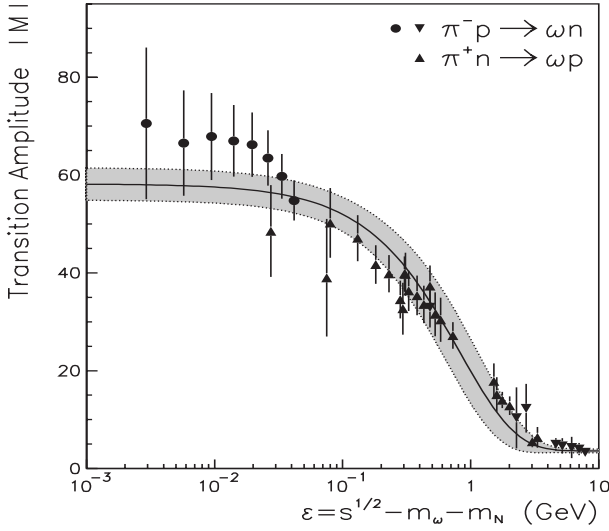
Table 1. The parameters of the approximation (3).

Reaction	M_0	M_1	γ
$\pi N \rightarrow \omega N$	3.6	54.6	1.21
$\pi N \rightarrow \phi N$	0.31	6.96	1.83
$pp \rightarrow pp\omega$	–	37.7	0.27

Since the data are not available for a comparison at exactly the same excess energies we fit the transition amplitudes by the function

$$|M_V| = M_0 + M_1 \exp\left(-\gamma\epsilon\right) \tag{3}$$

with the parameters given in Table 1. The solid lines in Figs. 1, 2 show the approximation (3) while the dashed areas indicate the uncertainty of the parameterization. Note, that the approximation is compatible with an almost constant transition amplitude for $\epsilon < 100$ MeV and reasonably reproduces the experimental results up to $\epsilon = 10$ GeV.

The resulting ratio of the $\pi N \rightarrow \omega N$ to $\pi N \rightarrow \phi N$ transition amplitudes is shown in Fig. 3a) by the solid line as a function of the excess energy ϵ. It is important to note that the ratio $R = |M_\omega|/|M_\phi|$ is almost constant within the given uncertainties up to $\epsilon = 10$ GeV, where the data are available.

Since the ω/ϕ ratio is always discussed as a constant, that is compared to the SU(3) predictions, we calculate the average value of $<R>$ in the range $0 < \epsilon < 10$ GeV. Figure 3b) shows the reduced χ^2 as a function of the constant

Fig. 1. Data on the $\pi N \rightarrow \omega N$ transition amplitude |M| as a function of the excess energy ϵ. The triangles show the data from [7] evaluated by (1) while the full dots show the data from [10] evaluated by (2). The solid line displays the approximation (3) while the dashed area illustrates the uncertainty of the fit.
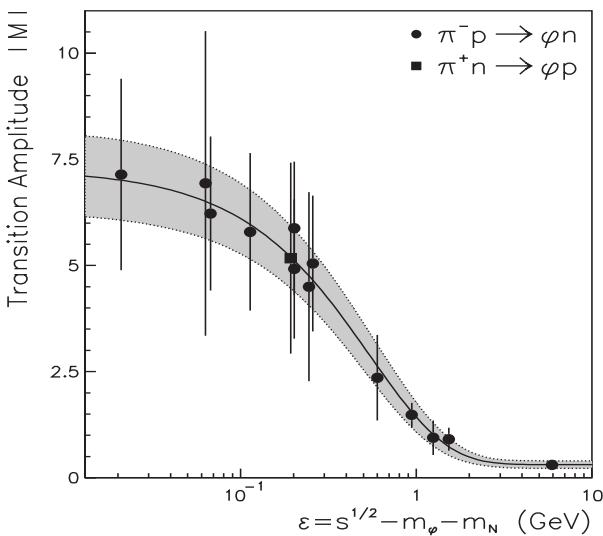

Fig. 2. Data on the $\pi N \rightarrow \phi N$ transition amplitude |M| as a function of the excess energy ϵ. The solid line shows the approximation (3) while the dashed area indicates the uncertainty of the fit.
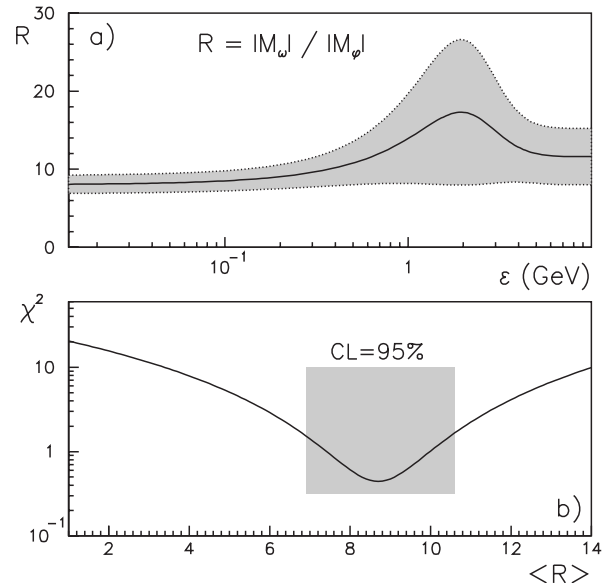

Fig. 3. a) The ratio R of the $\pi N \rightarrow \omega N$ and $\pi N \rightarrow \phi N$ transition amplitudes (solid line) and related uncertainty ΔR (dashed area) as a function of the excess energy ϵ. b) The reduced χ^2 for the approximation of the ratio R by a constant value $<R>$ (solid line) and the confidence interval (dashed area) for a confidence level of 95%.
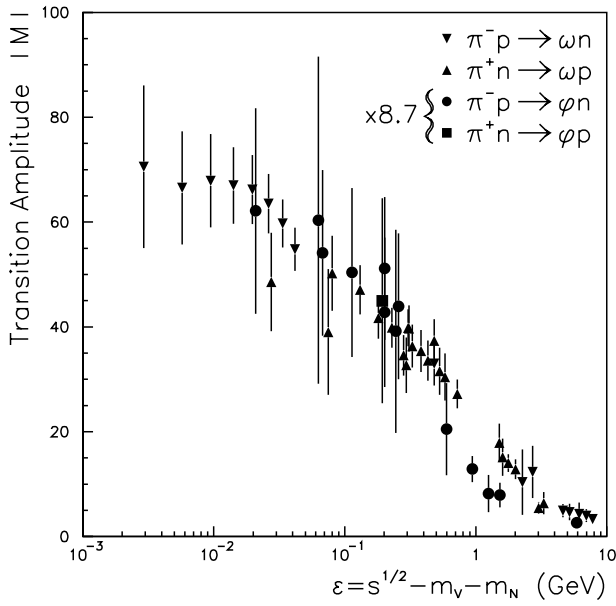
Fig. 4. Experimental results [7,10] for the $\pi N \to \omega N$ (triangles) and $\pi N \to \phi N$ (circles and squares) transition amplitude $|M|$ as a function of the excess energy ϵ, where the $\pi N \to \phi N$ amplitude is multiplied by a factor of $<R>=8.7$.

$<R>$, which approaches a minimum at

$$< R > = \frac{|M_{\pi N \to \omega N}|}{|M_{\pi N \to \phi N}|} = 8.7 \pm 1.8. \tag{4}$$

with the dispersion given for a 95% confidence level.

Furthermore, a visual way to control our estimate for $<R>$ is to compare the experimental data directly by multiplying the $\pi N \to \phi N$ amplitude by the factor $<R>$ as shown in Fig. 4. We note that four experimental points for the $\pi^- p \to \phi n$ reaction around $\epsilon = 1$ GeV deviate by a factor of $\simeq 1.8$ from the hypothesis applied. New experimental data with high accuracy are obviously necessary for a final conclusion about the ratio of the $\pi N \to \omega N$ and $\pi N \to \phi N$ reaction amplitudes.

3 ω and ϕ production in pp reactions

In our normalization the pp$\to$ppM total cross section for the production of an *unstable* meson with total width Γ is given as

$$\sigma = \frac{1}{2^8 \, \pi^3 \, s \, \lambda^{1/2}(s, m_N^2, m_N^2)} \int\limits_{m_{min}}^{\sqrt{s}-2m_N} \frac{1}{2\pi} \frac{\Gamma \, dx}{(x - m_V)^2 + \Gamma^2/4}$$

$$\times \int\limits_{4m_N^2}^{(\sqrt{s}-x)^2} |M|^2 \, \lambda^{1/2}(s, y, x^2) \, \lambda^{1/2}(y, m_N^2, m_N^2)$$

$$\times \, C^2(q = 0.5\sqrt{y - 4m_N^2}) \, \frac{dy}{y}, \tag{5}$$
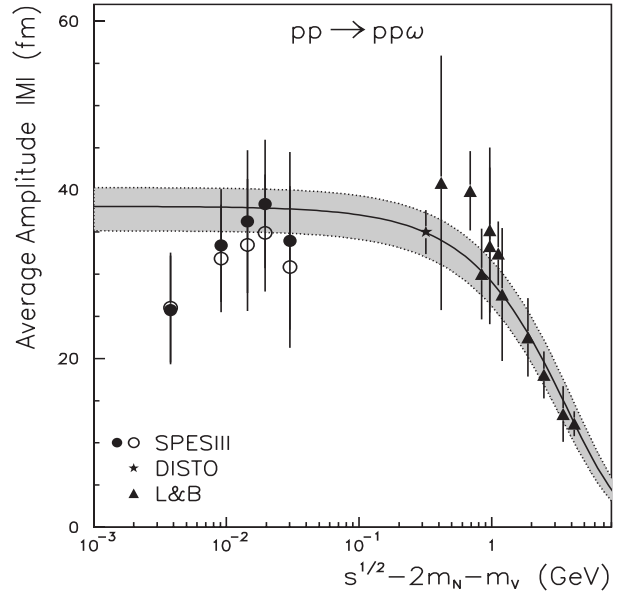

Fig. 5. The average amplitude $|M|$ for the pp$\to$ppω reaction as a function of the excess energy ϵ. The circles show the SPES-III [15] data evaluated with the FSI model from [16] (open circles) and from [17] (full circles). The triangles indicate the data from [7]; the star is our extrapolation for the DISTO experiment. The solid line shows the parameterization (3) while the dashed area indicates the related uncertainty.

where m_{min} is the minimal mass of the unstable particle and C(q) describes the final state interaction (FSI) between the nucleons [11–14].

Figure 5 shows the average production amplitude for the pp $\to$ ppω reaction evaluated by (5) from the data [7, 15] using the FSI models from [16,17][1]. We note that the uncertainty in the evaluation of the pp$\to$ppω production amplitude due to the different models of the FSI corrections is substantially smaller than the dispersion of the experimental results.

The pp$\to$ppω reaction amplitude evaluated from the data [7,15] is approximated by the function (3) with parameters given in Table 1 and is shown in Fig. 5 by the solid line. The dashed area in Fig. 5 indicates again the uncertainty of the approximation which was calculated with the error correlation matrix.

Recently the DISTO Collaboration reported an experimental result [6] on the ratio of the pp$\to$ppϕ and pp$\to$ppω total cross section at a beam energy of 2.85 GeV. For the further analysis we need the ϕ-meson production cross section explicitly, which can be obtained by normalization to the available data on ω-meson production [7,15]. Our extrapolation for the pp$\to$ppω production amplitude at 2.85 GeV is shown in Fig. 5 by the star and provides

$$\sigma(pp \to pp\omega) = 45 \pm 7 \ \mu b,$$

---

[1] A comparison between the different models for the final state interaction is presented in [17,18]

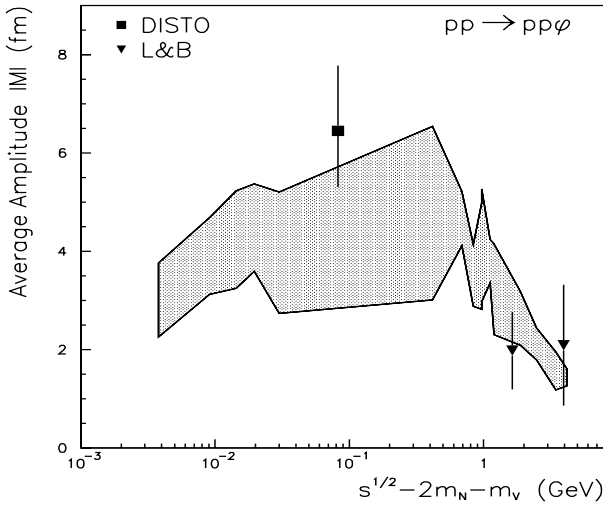**Fig. 6.** The average amplitude |M| for the pp→ppϕ reaction as a function of the excess energy ϵ. The square shows the result evaluated from the DISTO Collaboration [6] while the triangles were obtained from the data of [7]. The dashed area shows the experimental data on the pp→ppω amplitude, divided by the factor 8.5, where the data are connected by a line through their upper and lower error bars.

$$\sigma(pp{\to}pp\phi) = 0.17^{+0.07}_{-0.06}\ \mu b. \qquad (6)$$

Now the DISTO data point [6] for the pp→ppϕ total cross section can be used for the evaluation of the reaction amplitude. Figure 6 shows the experimental results for the average pp→ppϕ production amplitude as a function of the excess energy. Since there are only three experimen-

tal points we cannot perform a statistical analysis of the $|M_\omega|/|M_\phi|$ ratio similar to the $\pi N \to VN$ analysis. Note that the pp→ppϕ data are available only for $\epsilon{>}80$ MeV, where the FSI enhancement as well as the correction due to the final ϕ-meson width almost play no role.

Now, to compare the data one might take the ratio of the pp→ppω and pp→ppϕ amplitudes as a constant. The two experimental points at high energy give a ratio R $\simeq 8.5$. Figure 6 shows the pp $\to$ ppϕ production amplitude together with the pp $\to$ ppω experimental results divided by the factor 8.5. To illustrate the ϵ-dependence the data are simply connected by upper and lower lines through their error bars. Figure 7, furthermore, shows the data for the pp→ppϕ production amplitude using the fit (3) for the pp→ppω amplitude again divided by the factor 8.5. Here the DISTO data point sticks out from the error band to some extent. However, it is not clear if one might take the ω/ϕ ratio as independent on ϵ. As we already demonstrated for the $\pi N{\to}\omega N$ and $\pi N{\to}\phi N$ reactions, the $|M_\omega|/|M_\phi|$ ratio substantially depends on the excess energy for $\epsilon > 300$ MeV. In this sense, the DISTO result does not strictly contradict the pp→ppϕ data available at high energy.

Furthermore, since additional experimental results [19, 20] are available for the ratio of the ϕ/ω total or differential cross sections above 8 GeV bombarding energy, we also show this ratio calculated with (5) in Fig. 8 as a function of the incident proton energy.

We have performed a χ^2 fit to the available data on the ratio of the pp→ppϕ and pp→ppω cross sections with a constant ratio of the $|M_\omega|/|M_\phi|$ production amplitude and obtained the value of 8.5±1.0. Here the error is due to the parent standard deviation. The confidence level of the fit is below 50%. Again the DISTO result is not consistent with the constant ratio $|M_\omega|/|M_\phi|$=8.5. We mention that
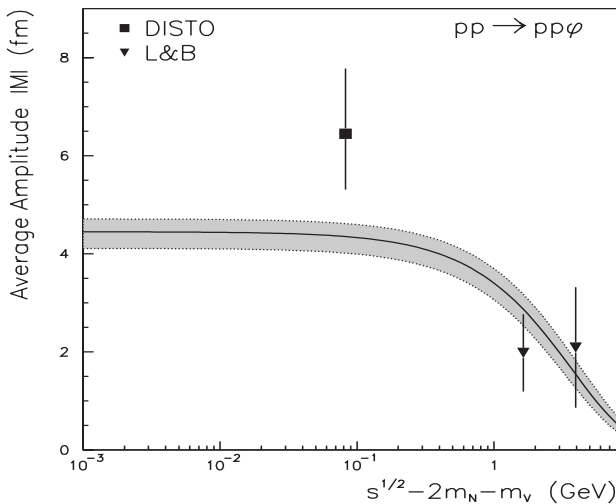

Fig. 7. The average amplitude |M| for the pp→ppϕ reaction as a function of the excess energy ϵ. The solid line shows the approximation (3) for the pp→ppω amplitude divided by the factor 8.5, while the dashed area is the uncertainty of the approximation with respect to the pp $\to$ ωpp data.

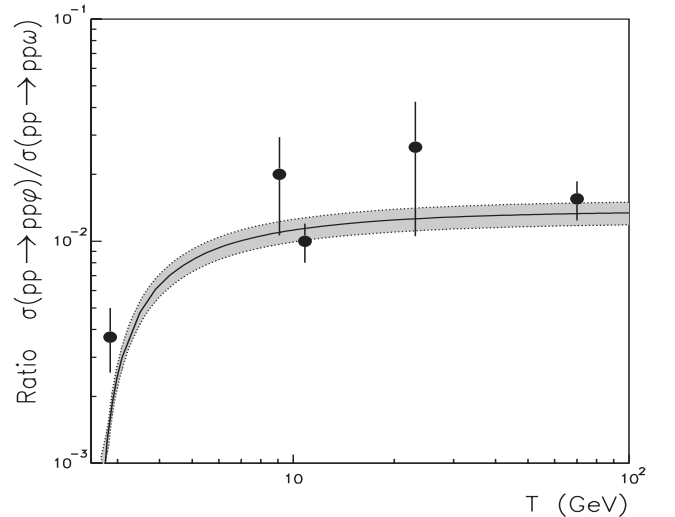**Fig. 8.** The ratio of the pp→ppϕ and pp→ppω cross sections as a function of the beam energy T. Experimental data are taken from [7, 6, 19, 20]. The solid line shows the result calculated with the energy independent ratio $|M_\omega|/|M_\phi|$=8.3, while the dashed area indicates the parent standard deviation.

the DISTO result on ϕ-meson production can be fixed by $|M_\omega|/|M_\phi|=5.72^{+1.01}_{-1.17}$ with the pp$\to$ppω amplitude taken from the approximation (3).

4 Theoretical interpretations

In general [21] the experimental results on the ϕ/ω ratio are compared to a constant as given by Lipkin [5],

$$R^2(\phi/\omega) = \frac{g^2_{\phi\rho\pi}}{g^2_{\omega\rho\pi}} = \frac{g^2_{\phi NN}}{g^2_{\omega NN}} = \frac{\sigma(\pi N \to \phi X)}{\sigma(\pi N \to \omega X)}$$

$$= \frac{\sigma(NN \to \phi X)}{\sigma(NN \to \omega X)} = \tan^2(\Delta\theta_V) = 4.2 \times 10^{-3}, \quad (7)$$

where $\Delta\theta_V$=3.7^0 [4] is the deviation from the ideal $\omega-\phi$ mixing angle. It is important to note, that (7) provides the ϕ/ω ratio for hadronic reactions which can be expressed by the diagrams shown in Fig. 9 that contain the V$\rho\pi$ and VNN vertices.

Furthermore, the ratio of the $\omega\rho\pi$ to $\phi\rho\pi$ coupling constant can be evaluated from the relevant partial decay width [22,23]. The $\phi\rho\pi$ coupling constant can be measured (as first proposed by Sakurai [22]) by the $\phi\to\rho\pi$ decay via

$$\Gamma_{\phi\to\rho\pi} = \frac{g^2_{\phi\rho\pi}}{16\pi^2 m_\phi^5} \int\limits_{2m_\pi}^{m_\phi-m_\pi} d\mu \; \lambda^{3/2}(m_\phi^2, \mu^2, m_\pi^2)$$

$$\times \frac{\mu^2 \, \Gamma_{\rho\to2\pi}(\mu)}{(\mu^2 - m_\rho^2)^2 + \mu^2\Gamma^2_{\rho\to2\pi}(\mu)}. \quad (8)$$

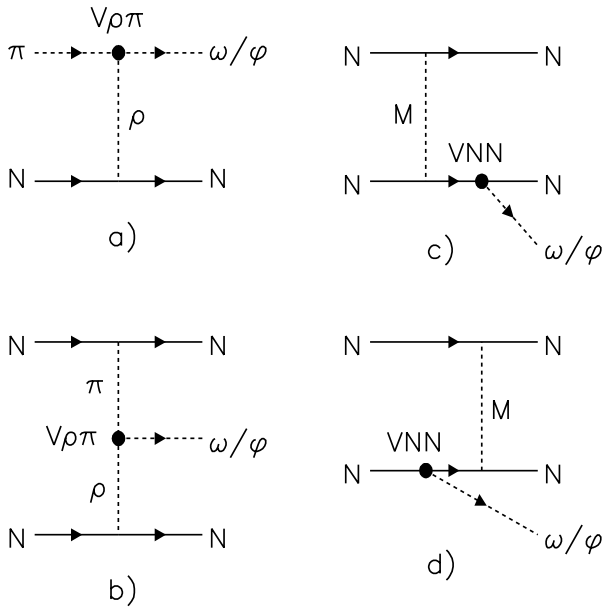**Fig. 9.** The diagrams for the πN$\to$VN (a) and NN$\to$VNN (b-d) reactions with V=ω, ϕ, that contain the V$\rho\pi$ and VNN vertices. Here M denotes the NN interaction in the initial or final state due to meson exchange.

Table 2. The coupling constants and their sources of extraction. The decay widths and masses are taken from [4]. Taking into account the contribution from the $\omega\to3\pi$ decay, which is 20% at 90% confidence level [4], we obtain $g_{\phi\rho\pi} \approx 1.1$.

Vertex	Source	Constant
$\phi\rho\pi$	$\Gamma(\phi \to \rho\pi)$	1.23 ± 0.05
$\rho\gamma$	$\Gamma(\rho \to e^+e^-)$	2.41 ± 0.12
$\rho\gamma$	$\Gamma(\rho \to \mu^+\mu^-)$	2.45 ± 0.15
$\omega\gamma$	$\Gamma(\omega \to e^+e^-)$	8.24 ± 0.24
$\omega\gamma$	$\Gamma(\omega \to \mu^+\mu^-)$	> 5.29
$\omega\rho\pi$	$\Gamma(\omega \to \pi^0\gamma)$	8.82 ± 0.50
$\omega\rho\pi$	$\Gamma(\rho \to \pi^0\gamma)$	12.32 ± 3.12
$\omega\rho\pi$	$\Gamma(\omega \to 3\pi)$	11.79 ± 0.19

Taking into account the energy dependence of the ρ-meson width and experimental numbers from the PDG [4] we obtain $g_{\phi\rho\pi}$ as shown in Table 2.

The separate $\omega\to\rho\pi$ decay is not energetically allowed and to determine the $\omega\rho\pi$ coupling constant Gell-Mann and Zachariasen [23] proposed to study the radiative decays $\omega\to\pi\gamma$ and $\rho\to\pi\gamma$. In their approach (see also the review of Meißner [24]) this process is dominated by the $\omega\rho\pi$ vertex with the intermediate vector meson coupled to the photon via vector dominance. The $\omega\rho\pi$ coupling constant can be measured by [23,25],

$$\Gamma(\omega \to \pi^0\gamma) = \frac{g^2_{\omega\rho\pi}}{96 \, m_\omega^5} \frac{\alpha}{\gamma_\rho^2} \left[m_\omega^2 - m_\pi^2\right]^3, \quad (9)$$

where α is the fine structure constant. Furthermore, a direct measurement of γ_ρ is possible by means of the vector meson decay into leptons [26]

$$\Gamma(\rho \to l^+l^-) = \frac{\pi}{3} \left[\frac{\alpha}{\gamma_\rho}\right]^2 \sqrt{m_V^2 - 4m_l^2} \left[1 + \frac{2m_l^2}{m_\rho^2}\right], \quad (10)$$

where m_ρ and m_l are the masses of the vector meson and lepton, respectively. In a similar way $g_{\omega\rho\pi}$ can be measured via the $\rho \to \pi^0\gamma$ decay. The relevant coupling constants obtained with the latest PDG fit to experimental data are listed in Table 2.

On the other hand, Gell-Mann, Sharp and Wagner [27] proposed to determine $g_{\omega\rho\pi}$ through the $\omega \to 3\pi$ decay assuming that the ω first converts into $\rho\pi$ followed by $\rho \to 2\pi$. The relation between the $\Gamma(\omega \to 3\pi)$ and $\omega\rho\pi$ coupling constants is given in [28]. A more elaborate analysis of the $\omega\to3\pi$ decay includes the four-point contact term due to the direct coupling between the ω-meson and three pions [24,29,25], however, the contribution from this anomalous coupling to $\Gamma(\omega \to 3\pi)$ is only about 10%. The analysis from Refs. [29,30] provides $g_{\omega\rho\pi}$=10.88.

Note that the mixing angle can also be determined by the ratio of the $\omega\to\pi^0\gamma$ and $\phi\to\pi^0\gamma$ radiative decay widths by applying vector dominance (9), which gives $g_{\omega\rho\pi}/g_{\phi\rho\pi}=$ 12.9$\pm$0.4. An alternative model [24,29,31] proposed a direct $\omega\pi\gamma$ coupling, instead of the vector dominance, where the ratio of $g_{\omega\rho\gamma}$ to $g_{\phi\rho\gamma}$ yields 16.8$\pm$1.0.

Both models predicts values close to the mixing angle θ_V=37^0, determined from the mass splitting in the vector-meson nonet, but depend on the vector dominance or direct coupling assumption. The direct $\phi\to\rho\pi$ decay is a more standard way, although it leads to a rather large uncertainty in the determination of the $\phi\rho\pi$ coupling.

To provide a graphical overview, Fig. 10 illustrates the ratio of the $\omega\rho\pi$ and $\phi\rho\pi$ coupling constants evaluated from the partial decay width. We also show the ratio given by the πN$\to$VN and pp$\to$Vpp data assuming that this ratio is energy independent. The DISTO result is shown separately and – as discussed above – is not consistent with the other data for pp reactions. However, within the present uncertainties the experimental results – as evaluated from all different sources – appear to be compatible; they all disagree with the SU(3) estimate based on the $\omega-\phi$ as given by the PDG [4].

We note, furthermore, that any production mechanism different from those in Fig. 9 will invalidate the overall scaling based on the $R^2(\phi/\omega)$ function [32,33]. For instance, as found in [34–40], two-step processes with intermediate $K\bar{K}$, $K^*\bar{K}$ $K^*\bar{K}^*$ states may contribute substantially to ϕ production in antiproton-proton annihilation. Certainly, such OZI allowed processes could have also an effect on ϕ-meson production in πN and NN reactions, but their actual contribution so far is unknown here. In view of Fig. 3a we speculate that their contribution should be rather low for excess energies $\epsilon \leq$300 MeV.
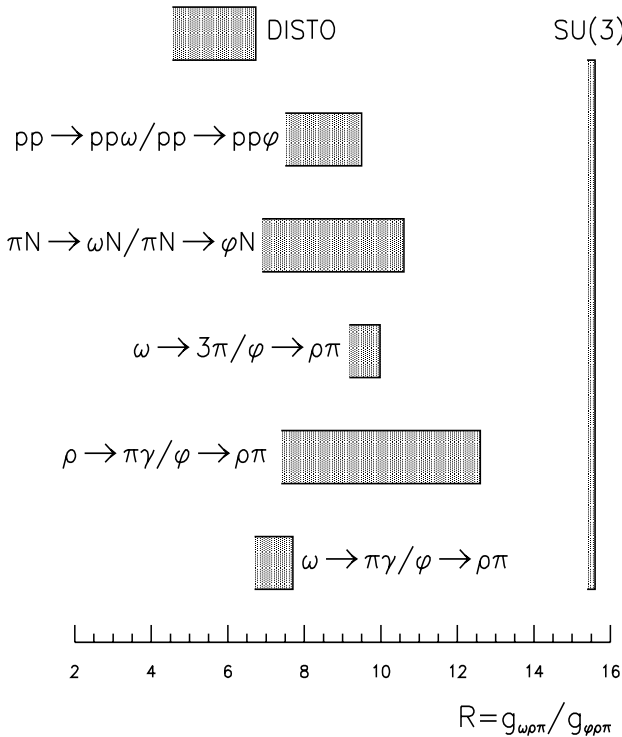
5 Summary

We have analyzed the experimental data available for ω and ϕ-meson production from πN and pp reactions and have evaluated the ratio of the reaction amplitudes. Indeed the experimental ϕ/ω ratio substantially deviates from the SU(3) estimate $R^2(\phi/\omega)$=4.2$\times10^{-3}$, which is based on the $\omega-\phi$ mixing angle of θ_V=39^0.

However, it is important to recall that this SU(3) estimate is given by the ratio of the $\phi\rho\pi$ to $\omega\rho\pi$ and ϕNN to ωNN coupling constants and is related only to the reaction mechanisms involving the relevant V$\rho\pi$ and VNN vertex. Obviously, any other production mechanism [34–40] as well as different form factors in the V$\rho\pi$ and VNN vertices will lead to a deviation of the experimental ratios from the simple scaling $R^2(\phi/\omega)$=4.2$\times10^{-3}$.

On the other side, by fitting the experimental ratio with a constant, our comparison of the πN and pp data with the ratio of the $\phi\rho\pi$ and $\omega\rho\pi$ coupling constant (as evaluated from the measured partial decay) shows an overall compatibility. The full analysis indicates that – within the experimental uncertainties – the data on the partial decays as well as on πN and pp reactions provide an average ratio $R^2(\phi/\omega)\simeq1.6\times10^{-2}$, which is close to the DISTO data point, however, disagrees with the SU(3) estimate based on the $\omega-\phi$ mixing angle of θ_V=39^0.

References

1. S. Okubo, Phys. Lett. **5**, (1963) 165
2. G. Zweig, CERN report TH-401 (1964)
3. J. Iizuka, Prog. Theor. Phys. Suppl. **38**, (1966) 21
4. Particle Data Group, Eur. Phys. J. C **3**, (1998) 1
5. H.J. Lipkin, Phys. Lett. B **60**, (1976) 371
6. F. Balestra et al., Phys. Rev. Lett. **81**, (1998) 4572
7. Landolt-Börnstein, *New Series* **I/12** (Springer, 1998)
8. R.P Feynman, *Theory of Fundamental Processes* (W.A. Benjamin Inc., New York, 1962)
9. C. Hanhart, A. Kudryavtsev, Eur. Phys. J. A **6**, (1999) 325
10. H. Karami et al., Nucl. Phys. B **154**, (1979) 503
11. K.M. Watson, Phys. Rev. **88**, (1952) 1163
12. A.B. Migdal, JETP **1**, (1955) 2
13. M. Gell-Mann and K.M. Watson, Ann. Rev. Nucl. Sci. **4**, (1954) 219
14. J.R. Taylor, *Scattering Theory* (Willey, New York, 1972)
15. F. Hibou et al., Phys. Rev. Lett. **83**, (1999) 492
16. B.L. Druzhinin, A. Kudryavtsev, and V.E. Tarasov, Z. Phys., A **359**, (1997) 205
17. A. Sibirtsev and W. Cassing, nucl-th/9904046
18. A. Sibirtsev and W. Cassing, Eur. Phys. J. A **2**, (1998) 333
19. M.W. Arenton et al., Phys. Rev. D **25**, (1982) 2241
20. S.V. Golovkin et al., Z. Phys. A **359**, (1997) 435
21. J. Ellis et al., Phys. Lett. B **353**, (1995) 319
22. J.J. Sakurai, Phys. Rev. Lett. **9**, (1962) 472

Fig. 10. The ratio of the $\omega\rho\pi$ and $\phi\rho\pi$ coupling constants evaluated from different sources of experimental data in comparison to the SU(3) prediction for $\Theta_V = 39^0$.

23. M. Gell-Mann and F. Zachariasen, Phys. Rev. **124**, (1961) 953
24. Ulf-G. Meißner, Phys. Rep. **161**, (1988) 213
25. Ö. Kaymakcalan, S. Rajeev and J. Schechter, Phys. Rev. D **30**, (1984) 594
26. Y. Nambu and J.J. Sakurai, Phys. Rev. Lett. **8**, (1962) 79
27. M. Gell-Mann, D. Sharp and W.G. Wagner, Phys. Rev. Lett. **8**, (1962) 261
28. P. Lichard, Phys. Rev. D **49**, (1994) 5812
29. F. Klingl, N. Kaiser and W. Weise, Z. Phys. A **356**, (1996) 193
30. F. Klingl, private communication
31. P. Jain et al., Phys. Rev. D **37**, (1998) 3252
32. K. Nakayama et al., Phys. Rev. C **60**, (1999) 055209
33. K. Nakayama et al., Phys. Rev. C **57**, (1998) 1580
34. M.P. Locher, Y. Lu and B.S. Zou, Z. Phys. A **347**, (1994) 281
35. D. Buzatu and F.M. Lev, Phys. Lett. B **329**, (1994) 143
36. V. Mull, K. Holinde and J. Speth, Phys. Lett. B **334**, (1994) 295
37. D. Buzatu and F.M. Lev, Phys. Rev. C **51**, (1995) 2893
38. O. Gortchakov, M.P. Locher, V.E. Markushin and S. von Rotz, Z. Phys. A **353**, (1996) 447
39. A.V. Anisovich and E. Klempt, Z. Phys. A **354**, (1996) 197
40. V.E. Markushin and M.P. Locher, Eur. Phys. J. A **1**, (1998) 91